Electronic supplementary information

From Tanghulu-like to Cattail-like SiC Nanowire Architectures: Interfacial Design of Nanocellulose Composites toward Highly Thermal Conductivity

Bai Xue[a,b][#], Shengdu Yang[a#], Xin Sun[a], Lan Xie[a,b]*, and Qiang Zheng[c].*

a. Department of Polymer Materials and Engineering, College of Materials and Metallurgy, Guizhou University, Guiyang 550025, China.

b. National Engineering Research Center for Compounding and Modification of Polymer Materials; National and Local Joint Engineering Research Center for Functional Polymer Membrane Materials and Membrane Processes, Guiyang 550014, China.

c. College of Polymer Science and Engineering, Zhejiang University, Hangzhou 310000, China.

**Corresponding Author: Bai Xue,* bxue@gzu.edu.cn *or* xueb126@126.com

Lan Xie, mm.lanxie@gzu.edu.cn *or* lancysmile@163.com

 # Shengdu Yang and Bai Xue contributed equally to this work.

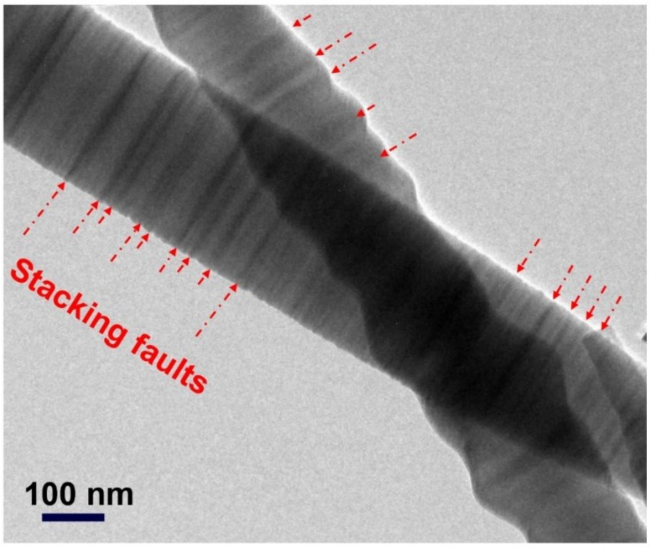

Figure S1. TEM image of the bare SiCNWs

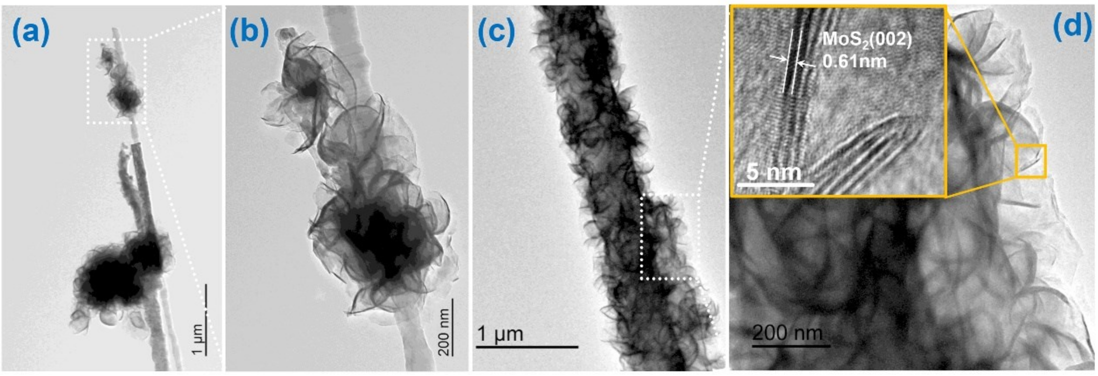

Figure S2: (a) and (b) TEM images of L-MoS_2-SiCNWs. (c) and (d) TEM images of H-MoS_2-SiCNWs.

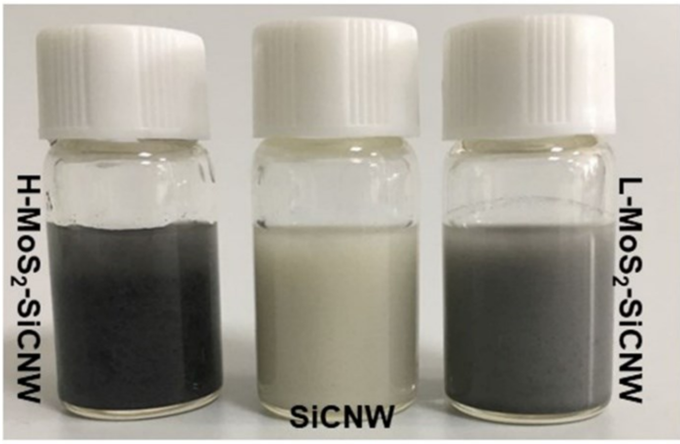

Figure S3. Digital photos showing the dispersion sate of synthetic nanohybrids

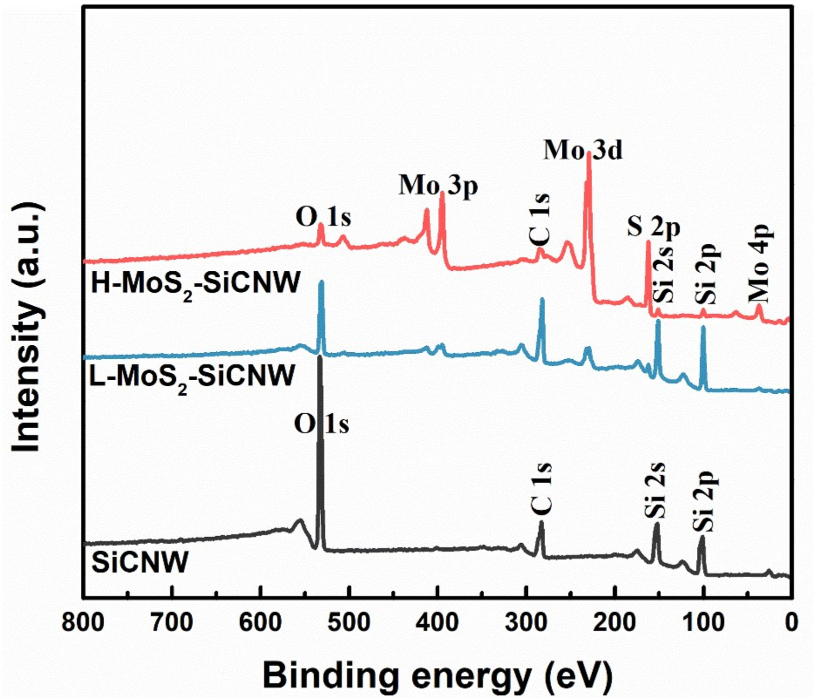

Figure S4: Full-range XPS spectra of bare SiCNW, L-MoS_2-SiCNW, and H-MoS_2-SiCNW hybrids.

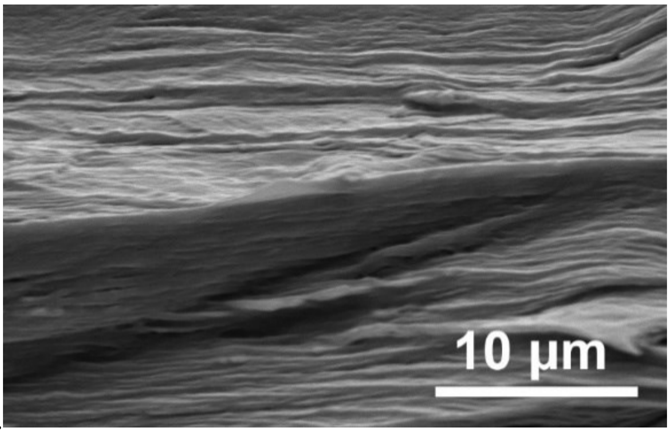

Figure S5: The cross-section SEM image of pure CNF film.

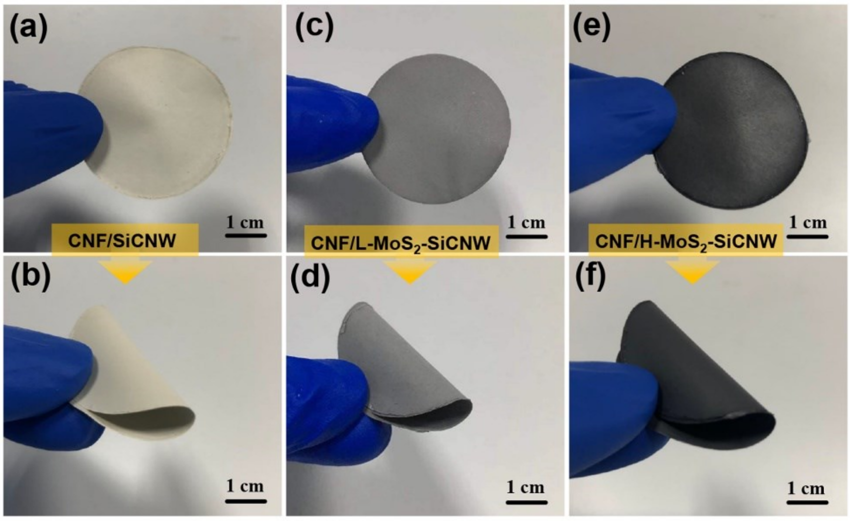

Figure S6: Digital photos of (a, b) CNF/SiCNW, (c, d) CNF/L-MoS_2-SiCNW and (e, f) CNF/H-MoS_2-SiCNW films, respectively.

Table S1: Comparison with TC and TCE values of previously reported composites

Ref.	*Fillers*	*Matrix*	*Loading (wt%)*	*TC ($W\ m^{-1}K^{-1}$)*		*TCE (%)*	*Testing way*
				$TC_{\perp}$	*$TC_{//}$*		
S1	BNNS	Epoxy	~40	◇0.7	◆6.54	3170	Steady-state
S2	PMMA-g-FCNT	PMMA	15	◇~0.35	◆1.16	510	Laser flash
S3	ND	CNF	0.5	◇0.118	◆9.82	775	Laser flash
S4	*f*-BNNS	CNF	70	◇~0.6	◆12.79	699	Laser flash
S5	FCNT	NFC	35	◇0.83	◆14.1	729	Laser flash
S6	MgO@rGO	NFC	20	◇0.32	◆6.17	630	Laser flash
S7	BNNPs	NFC	40	◇~0.5	◆20.64	985	Laser flash
S8	GNP	PDA	44.4	◇0.69	◆13.42	-	Laser flash
S9	rGO	NFC	30	◇0.07	◆6.17	550	Laser flash
S10	CPGO	CNF	70	◇~0.3	◆12.75	165	Laser flash
S11	BNNS@PDA	ANF	50	◇0.62	◆3.94	196	Steady-state
S12	BNNS-OH	CNF	75	◇0.45	◆15	235	Laser flash
This work	H-MoS_2-SiCNW	CNF	40 (22.5 vol%)	☆0.68	★19.76	1408	Laser flash

According to our defined the rule of mixtures (Eq. (S1)), the thermal conductivity of L/H-MoS_2-SiCNW ($K_{p(mix)}$) can be calculated from,

$$K_{p(mix)} = K_{SiCNW} f + K_{MoS_2}(1-f) \quad \text{(S1)}$$

where K_{MoS2}=82 $Wm^{-1}K^{-1}$, K_{SiCNW}=120 $Wm^{-1}K^{-1}$ and f is the volume fraction of SiCNW in MoS_2/SiCNW hybrid.

$$\rho_{SiCNW} = 3.21 g/cm^3, \rho_{MoS2} = 4.80 g/cm^3$$

The exact content of MoS_2 is 78.6 wt% (64.8 vol%) in L-MoS_2-SiCNWs and 97.0 wt% (95.6 vol%) in H-MoS_2-SiCNWs.

Thus, f = 35.2 vol% (L-MoS_2-SiCNW), f = 4.4 vol% (H-MoS_2-SiCNW)

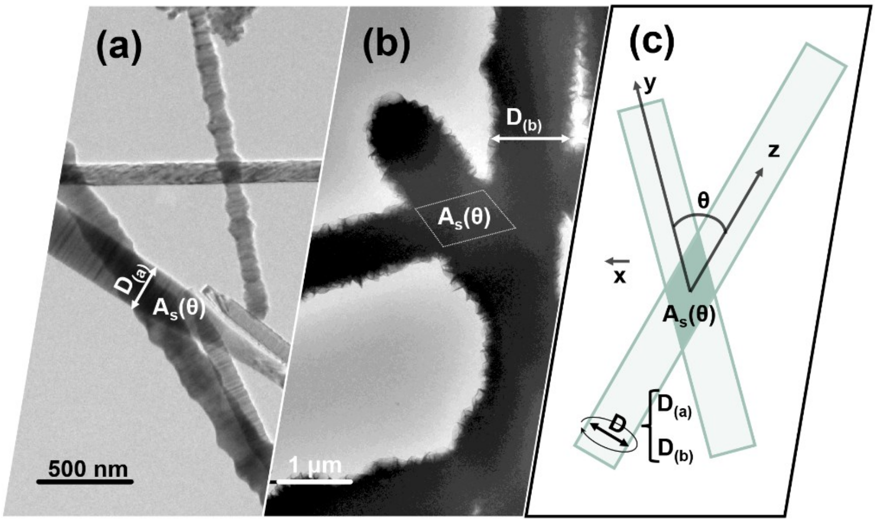

Figure S7: The average overlap area ($\bar{A}_s$) between adjacent fillers for (a) bare SiCNWs and (b) H-MoS_2-SiCNWs. (c) Schematic diagram of the average overlap area ($\bar{A}_s$).

$$\bar{A}_s = \frac{2D^2}{\pi}\left[\ln\left(\sin\frac{\theta}{2}\right) - \ln\left(\cos\frac{\theta}{2}\right)\right]_0^{\frac{\pi}{2}} \quad \text{(S2)}$$

$$A_{s,c} = \frac{D_{(a,b)}^2}{\sin(\theta_c)} \quad \text{(S3)}$$

$$\bar{A}_s = \frac{2D^2}{\pi}\delta(p) \quad (S4)$$

$$\delta(p) = \ln\left[\frac{\sqrt{1+p^{-1}}+\sqrt{1-p^{-1}}}{\sqrt{1+p^{-1}}-\sqrt{1-p^{-1}}}\right] \quad (S5)$$

$\bar{A}_s = 5.46 \times 10^{-14}$ m^2 for bare SiCNWs and $\bar{A}_s = 3.19 \times 10^{-12}$ m^2 for H-MoS_2-SiCNWs.

Table S2: The values of V_c, K_o, and *t(p)* for CNF/SiCNW and CNF/H-MoS_2-SiCNW.

Sample	V_c	K_0	*t(p)*
CNF/SiCNW	8.7×10^{-4}	5.95	0.23
CNF/H-MoS_2-SiCNW	8.0×10^{-3}	6.79	0.50

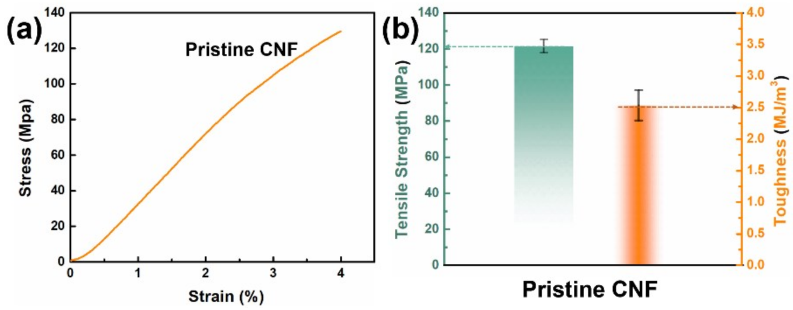

Figure S8. (a) Typical strain-stress curve and (b) Tensile strength and toughness of pure CNF film.

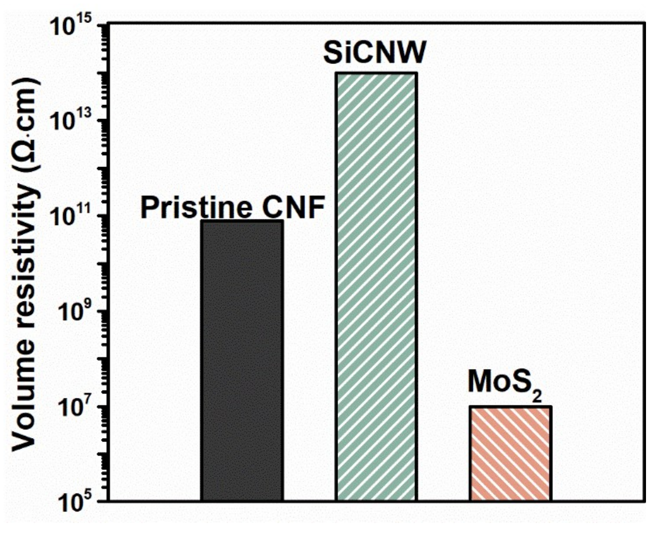

Figure S9. Volume resistivities of Pristine CNF, SiCNW, and MoS_2

As shown in Figure S9, the volume resistance of pure SiCNWs (2.1×10^{14} Ω·cm) is far higher than that of pure CNF film (7.9×10^{10} Ω·cm). Thus, the volume resistance of CNF/SiCNW is largely increased to 2.4×10^{13} Ω·cm with the introduction of 22.5 vol% SiCNWs. However, the volume resistance of MoS_2 is as low as 1.3×10^{7} Ω·cm. Hence, with the introduction of SiCNW hybrids (L-MoS_2-SiCNW and H-MoS_2-SiCNW), the volume resistances of CNF/L-MoS_2-SiCNW and CNF/H-MoS_2-SiCNW are moderately reduced to 1.7×10^{13} Ω·cm and 4.1×10^{12} Ω·cm, respectively, which is still superior to that of pure CNF film.

References

S1. J. Han, G. Du, W. Gao and H. Bai, *Adv. Funct. Mater.*, 2019, **29**, 1904c12.

S2. X. Wang and P. Wu, *Chem. Eng. J.*, 2019, **369**, 272-279.

S3. N. Song, S. Cui, X. Hou, P. Ding and L. Shi, *ACS Appl. Mater. Interfaces*, 2017, **9**, 40766-40773.

S4. K. Wu, J. Fang, J. Ma, R. Huang, S. Chai, F. Chen and Q. Fu, *ACS Appl. Mater. Interfaces*, 2017, **9**, 30035-30045.

S5. X. Wang and P. Wu, *ACS Appl. Mater. Interfaces*, 2018, **10**, 34311-34321.

S6. M. Ma, L. Xu, L. Qiao, S. Chen, Y. Shi, H. He and X. Wang, *Chem. Eng. J.*, 2019, **385**, 123714.

S7. Q. Li, Z. Xue, J. Zhao, C. Ao, X. Jia, T. Xia, Q. Wang, X. Deng, W. Zhang and C. Lu, *Chem. Eng. J.*, 2020, **383**, 123101.

S8. F. Luo, K. Wu, J. Shi, X. Du, X. Li, L. Yang and M. Lu, *J. Mater. Chem. A*, 2017, **5**, 18542-18550.

S9. N. Song, D. Jiao, P. Ding, S. Cui, S. Tang and L. Shi, *J. Mater. Chem. C*, 2016, **4**, 305-314.

S10. Y. Liu, M. Lu, Z. Hu, L. Liang, J. Shi, X. Huang, M. Lu and K. Wu, *Chem. Eng. J.*, 2019, **383**, 122733.

S11. T. Ma, Y. Zhao, K. Ruan, X. Liu, J. Zhang, Y. Guo, X. Yang, J. Kong and J. Gu, *ACS Appl. Mater. Interfaces*, 2020, 12, 1677-1686.

S12. Z. Hu, S. Wang, G. Chen, Q. zhang, K. Wu, J. Shi, L. Liang and M. Lu, *Compos. Sci. Technol.*, 2018, **168**, 287-295.